Iraqi Journal of Science, 2023, Vol. 64, No. 5, pp: 2354-2367
DOI: 10.24996/ijs.2023.64.5.21

ISSN: 0067-2904

Analytical Investigation of Electroosmotically Regulated Peristaltic Propulsion of Cu-water Nanofluid Through a Microtube

Adil Wahid Butt[1], Noreen Sher Akbar[2], Dharmendra Tripathi[3], Javaria Akram[4]
[1]*Department of Mathematics and Statistics, Riphah International University, Islamabad, Pakistan*
[2]*DBS&H, CEME, National University of Sciences and Technology, Islamabad, Pakistan*
[3]*Department of Mechanical Engineering, Manipal University Jaipur, Rajasthan-303007, India*
[4]*School of Natural Sciences, National University of Sciences and Technology, Islamabad, Pakistan*

Received: 11/7/2021 Accepted: 19/2/2022 Published: 30/5/2023

Abstract
The purpose of this investigation is to determine and analyze the fluid inertia of electroosmotic flow on the Cu-water nanofluids by peristaltic transport. Fluid flow properties and heat transfer characteristics are studied for aqueous ionic nanofluids through a vertical microtube of a constant radius. Streamlines are plotted for the governing fluid flow.

Keywords: Electroosmosis; Peristalsis; Nanofluid; Cu-Water; Exact solutions.

1. Introduction

Peristalsis is a phenomenon in which wall contraction and expansion induce the flow motion in the flow geometry along the length of the channel. This peristaltic wall movement leads to unidirectional fluid flow. This fluid transport mechanism has been adopted in industrial, physiological, and medical applications. In this regard, a large number of various rheological fluid flow models and flow geometries have been thoroughly explored both theoretically and experimentally [1-5]. Moreover, peristaltic transport is vastly considered for endoscopy analysis of blood flow [6], and for micro-pumping of a portable artificial kidney [7]. The time-dependent viscous flow is analyzed by Tripathi et al. [8], where they demonstrated the electroosmotic act as an external pumping actuator that regulates the peristaltic transport of viscous fluid.

Electroosmotic flow is a type of flow in which the electric field is in the direction of the tangent to the electrical double layer (EDL). In the diffuse layer, the body force is induced on the charged ions that are known as electroosmotic force (EOF). The motion of the fluid over a fixed charged surface caused by an electroosmotic flow has earned tremendous vigilance in recent years. In this regard, Reuss [9] addressed the electrokinetic flow phenomena on porous clay. Helmholtz [10] encompassed the EDL theory which averred the relationship between electric field and flow parameters for electrokinetic transport. Furthermore, various models with the electroosmotic flow have been established to study the influence of flow inertial, pressure distribution, and velocity distribution in the porous medium, capillary tube, or any other fluid channel [11-15].

Electroosmotic flow has a broad range of applications in the area of biological and biomedical systems. The equation governing the electroosmotic peristaltic flow is the

*Email: adil.maths@nutech.edu.pk

combination of Navier stokes and electrokinetic equations. The generic phenomena of electroosmosis controls and stabilizes the two-fluid interface that is induced by the pressure gradient. Prakash et al. [16] presented the heat characteristics of blood flow induced by electroosmosis. This study scrutinizes the dynamics of a nanofluid through peristaltic transport. Nanofluids are the new symbol of technology. A major application of nanofluids is in the heat transfer processes in the industry, because nanofluids have excellent temperature enhancement properties. The peristaltic transport of nanofluids in a non-uniform channel is discussed by Noreen et al. [17]. Bachok et al. [18] examined the boundary-layer flow of nanofluids, where the surface is the same and in opposite directions. Various researchers across the globe [19-23] have done theoretical studies dealing with the electroosmotic flow in nanofluids. They analyzed the effects of flow inertia, pressure gradient and temperature profiles in different flow regimes.

Most of the research in nanofluids is based on heat dissipation, which is required in many diverse industrial processes. Since nanofluids have the potential of bringing effective thermal conductivity and stability in industrial processes, therefore, heat transfer fluids consist of suspended nanoparticles to improve thermal conductivity. Mustafa et al. [24] discussed the peristaltic flow of nanofluids with compliant walls. Tripathi and Beg [25] examined the drug delivery system through the peristaltic flow of nanofluids. Many authors studied and investigated the influence of various types of nanoparticles on the peristaltic flows. The scrutiny of the Al_2O_3-water nanofluids flow in a micro Tesla valve was done by Qian et al. [26]. Their chemical approach is a novel technique for growing nanostructures in the nanochemistry area. This technique leads to precise control of the condition and produces monodispersed nanostructures. Copper (cu) nanoparticles in the fluid are of considerable interest for use as coolants and thier application in heat exchange. In this regard, literature is available including enhancement of thermal conductivity with cu-water [27-30].

The motivation behind the present attempt is to inspect the effects of cu-water nanofluids in the plumb duct in the existence of electroosmotic flow, which has not been discussed before. We also discuss the impact of the nanoparticles to illustrate the peristaltic transport in the micro plum duct. The present model is conferred using the long wavelength and low Reynolds number approximation.

2. Formulation of the Problem

Consider an electroosmosis regulated peristaltic fluid flow of aqueous ionic nanofluid through a vertical microtube of constant radius d. The copper nanoparticles are suspended in the base fluid to prepare the nanofluid. The fluid flow is driven by the combined effect of electroosmosis and peristaltic pumping. Further, it is assumed that ionic species present in the aqueous ionic solution have equal valence which means the solution is symmetric. These ionic species are set into motion by enforcing an external electric field around the electric double layer carrying nearby fluid molecules with them.

The fluid flow is moving inside a plumb duct under the influence of gravitational force. The peristaltic pumping is generated by the propagation of the sinusoidal waves along the walls of the tube with constant wave speed c and wavelength λ. The cylindrical coordinates system $(\bar{r},\ \bar{z},\ \bar{t})$ is found to be more suitable to formulate the fluid flow problem in which $\bar{r}$ and $\bar{z}$ represent the radial and axial direction respectively and the time is represented by $\bar{t}$. The deformation in the tube walls is physically shown in Figure 1 and mathematically is represented as: -

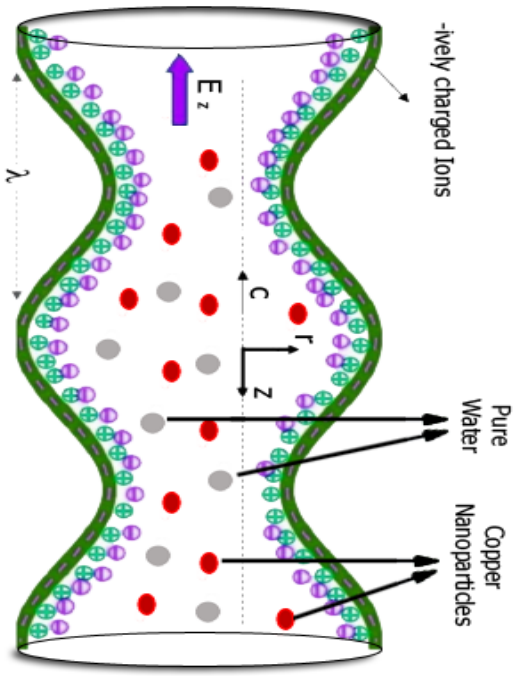

Figure 1: Flow geometry of the problem.

where the boundary is given by: -

$$r = \pm\bar{H}(\bar{x},\bar{t}) = \pm d \pm m\, sin\left(\frac{2\pi}{\lambda}(\bar{z} - c\bar{t})\right), \tag{1}$$

here d specifies the radius of the tube and m is the amplitude of the wave. The periodic expression $sin\left(\frac{2\pi}{\lambda}(\bar{z} - c\bar{t})\right)$ represents the deformation in the tube walls.

3. Governing Equations

The governing set of equations formulated under the effect of mixed convection, heat source, and electroosmosis are given as:

$$\frac{\partial\widetilde{U}}{\partial\tilde{R}} + \frac{\widetilde{U}}{\tilde{R}} + \frac{\partial\widetilde{W}}{\partial\tilde{Z}} = 0, \tag{2}$$

$$\rho_{nf}\left(\frac{\partial\widetilde{U}}{\partial\tilde{t}} + \widetilde{U}\frac{\partial\widetilde{U}}{\partial\tilde{R}} + \widetilde{W}\frac{\partial\widetilde{U}}{\partial\tilde{Z}}\right) = -\frac{\partial\tilde{P}}{\partial\tilde{R}} + \mu_{nf}\left(\frac{\partial^2\widetilde{U}}{\partial\tilde{R}^2} + \frac{1}{\tilde{R}}\frac{\partial\widetilde{U}}{\partial\tilde{R}} - \frac{\widetilde{U}}{\tilde{R}^2} + \frac{\partial^2\widetilde{U}}{\partial\tilde{Z}^2}\right) + \rho_e E_{\tilde{R}}, \tag{3}$$

$$\rho_{nf}\left(\frac{\partial\widetilde{W}}{\partial\tilde{t}} + \widetilde{U}\frac{\partial\widetilde{W}}{\partial\tilde{R}} + \widetilde{W}\frac{\partial\widetilde{W}}{\partial\tilde{Z}}\right) = -\frac{\partial\tilde{P}}{\partial\tilde{Z}} + \mu_{nf}\left(\frac{\partial^2\widetilde{W}}{\partial\tilde{R}^2} + \frac{1}{\tilde{R}}\frac{\partial\widetilde{W}}{\partial\tilde{R}} + \frac{\partial^2\widetilde{W}}{\partial\tilde{Z}^2}\right) + \rho_e E_{\tilde{Z}} + (\rho\gamma)_{nf}(\tilde{T} - T_0), \tag{4}$$

$$(\rho c)_{nf}\left(\frac{\partial\tilde{T}}{\partial\tilde{t}} + \widetilde{U}\frac{\partial\tilde{T}}{\partial\tilde{R}} + \widetilde{W}\frac{\partial\tilde{T}}{\partial\tilde{Z}}\right) = k_{nf}\left(\frac{\partial^2\tilde{T}}{\partial\tilde{R}^2} + \frac{1}{\tilde{R}}\frac{\partial\tilde{T}}{\partial\tilde{R}} + \frac{\partial^2\tilde{T}}{\partial\tilde{Z}^2}\right) + Q_0, \tag{5}$$

in which $E_{\tilde{R}}$ and $E_{\tilde{Z}}$ specify the electric body forces in the radial and the axial direction respectively, $\widetilde{U}$ is the velocity component in the radial direction, $\widetilde{W}$ is the velocity in the axial direction, $\tilde{T}$ is the temperature of the fluid, k_{nf} is the effective thermal conductivity of nanofluid, Q_0 is the heat source parameter, $(\rho c)_{nf}$ is the specific heat of the nanofluid, ρ_{nf} and μ_{nf} are the effective density and the viscosity of nanofluid respectively, $(\rho\gamma)_{nf}$ is the thermal expansion coefficient of nanofluid and ρ_e is the eclectic number density of electrolyte solution.

From the general mixture rule, the effective density, specific heat, and thermal expansion coefficient of Cu-water nanofluid are determined. The relation of the Brinkman and Maxwell model is employed to specify the viscosity and thermal conductivity of nanofluid as follows:

$$\begin{gathered}\rho_{nf} = (1-\phi)\rho_f + \phi\rho_p,\ \mu_{nf} = \frac{\mu_f}{(1-\phi)^{2.5}},\\ (\rho c_p)_{nf} = (1-\phi)(\rho c_p)_f + \phi(\rho c_p)_f,\ \alpha_{nf} = \frac{k_{nf}}{(\rho c_p)_{nf}},\\ (\rho\gamma)_{nf} = (1-\phi)(\rho\gamma)_f + \phi(\rho\gamma)_p,\\ \frac{k_f}{k_{nf}} = \frac{k_p + 2k_f + 2\phi(k_f - k_p)}{k_p + 2k_f - 2\phi(k_f - k_p)}\end{gathered} \tag{6}$$

where ϕ designates the nanoparticle volume fraction, the subscript f denotes the properties of the base fluid and p denotes the solid particle properties. The distribution of an electric potential within the fluid medium is described by the Poisson equation as follows:

$$\nabla^2\tilde{\varphi} = \frac{\partial^2\tilde{\varphi}}{\partial\tilde{R}^2} + \frac{1}{\bar{r}}\frac{\partial\tilde{\varphi}}{\partial\tilde{R}} + \frac{\partial^2\tilde{\varphi}}{\partial\tilde{Z}^2} = -\frac{\rho_e}{\varepsilon_r\varepsilon_0}. \tag{7}$$

Here ε_r represents the relative permittivity of the medium, ε_0 is the permittivity of the vacuum and electric number density in terms of the number density of cations n^+ and the anions n^- is described as:

$$\rho_e = ez(n^+ - n^-). \tag{8}$$

Defining the transformation of velocity components and the coordinates from the stationary frame to the wave frame (moving frame of reference), to observe the steady fluid flow, as:

$$\begin{gathered}\bar{z} = \tilde{Z} - c\tilde{t}, \bar{r} = \tilde{R}, \overline{w} = \widetilde{W} - c,\\ \bar{u} = \widetilde{U}, \bar{p}(\bar{r},\bar{z}) = \tilde{P}\left(\tilde{R},\tilde{Z},\tilde{t}\right).\end{gathered} \tag{9}$$

We introduce the following non-dimensional parameters to simplify the flow problem:

$$\begin{gathered}r = \frac{\bar{r}}{\lambda}, z = \frac{\bar{z}}{d}, p = \frac{\bar{p}d^2}{\mu_f c\,\lambda}, n = \frac{\tilde{n}}{n_0}, Re = \frac{\rho_f cd}{\mu_f}, \bar{\Psi} = \frac{\Psi}{cd},\\ h = \frac{\bar{H}}{d}, Pr = \frac{\mu_f c_p}{k_f}, \delta = \frac{d}{\lambda}, \theta = \frac{\bar{T} - T_0}{T_0}, G_r = \frac{\rho_f g\gamma_f d^2 T_0}{\mu_f c},\\ U = -\frac{\varepsilon_0\varepsilon_r k_f \hat{T}_{avg} E_z}{ez\mu_f c}, k = \sqrt{\frac{2n_0 e^2 z^2 d^2}{\varepsilon_0\varepsilon_r k_f \hat{T}_{avg}}} = \frac{d}{\lambda_d}, \varphi = \frac{ez\tilde{\varphi}}{k_f\hat{T}_{avg}},\\ \beta = \frac{Q_0 d^2}{T_0 k_f}, L = \frac{(\rho\gamma)_{nf}}{(\rho\gamma)_f}.\end{gathered} \tag{10}$$

and then applying the lubrication linearization theory of long wavelength and the low Reynolds number, we are left with simplified set of equations:

$$\frac{\partial p}{\partial r} = 0, \tag{11}$$

$$\frac{dp}{dz} = \frac{\mu_{nf}}{\mu_f}\frac{1}{r}\frac{\partial}{\partial r}\left(r\frac{\partial w}{\partial r}\right) + G_r\,L\,\theta + U\frac{1}{r}\frac{\partial}{\partial r}\left(r\frac{\partial\varphi}{\partial r}\right), \tag{12}$$

$$\frac{1}{r}\frac{\partial}{\partial r}\left(r\frac{\partial\theta}{\partial r}\right)+\beta\frac{k_f}{k_{nf}}=0, \tag{13}$$

$$\frac{1}{r}\frac{\partial}{\partial r}\left(r\frac{\partial\varphi}{\partial r}\right)=k^2\left(\frac{n^- - n^+}{2}\right), \tag{14}$$

where U designates the Helmholtz-Smoluchowski velocity or electroosmotic velocity parameter, G_r is the Grashof number, β is the dimensionless heat source parameter, θ represents the dimensionless temperature parameter, and k is the Debye length parameter.
The local ionic distribution of ionic species can be specified by linearizing the Boltzmann distribution for low zeta potential which accurately estimates the electric potential that is established in the fluid medium without even increasing the difficulty of the flow problem as for most of the electrolyte solution, the generated electric potential lies in the range that is less than or equal to 25mV.

$$n^{\pm}=e^{\mp\varphi}, \tag{15}$$

Using equation (15) in (14), we get the linearized Poisson-Boltzmann paradigm [31] as:

$$\frac{1}{r}\frac{\partial}{\partial r}\left(r\frac{\partial\varphi}{\partial r}\right)=k^2\sinh(\varphi), \tag{16}$$

which can be further simplified under Debye-Hückel approximation [31] i.e. $\sinh(\varphi)\approx\varphi$ as:

$$\frac{1}{r}\frac{\partial}{\partial r}\left(r\frac{\partial\varphi}{\partial r}\right)=k^2\varphi. \tag{17}$$

The dimensionless form of the no-slip boundary conditions for velocity temperature and electric potential enforced along the tube walls is given by:

$$\begin{aligned} &\varphi=\xi, \quad w=-1, \quad \theta=0, \quad at \quad r=h=1+\varepsilon\sin(2\pi z),\\ &\frac{\partial\varphi}{\partial r}=0, \quad \frac{\partial w}{\partial r}=0, \quad \frac{\partial\theta}{\partial r}=0, \quad at \quad r=0. \end{aligned} \tag{18}$$

4. Solution Profiles

An analytic expression for velocity profile, temperature distribution, and electric potential can be obtained by integrating equations (12-13) and (17) with the help of appropriate boundary conditions. The resulting velocity profile, temperature distribution, and electric potential are given as:-

$$w(r,z)=\frac{(h^2-r^2)\left(G_r\,L\,\frac{k_f}{k_{nf}}\,\beta(3h^2-r^2)-16\frac{dp}{dz}\right)+64\left(U\xi-\frac{\mu_{nf}}{\mu_f}\right)-64\,U\,\xi\,\frac{\mathrm{I}_0(r\,k)}{\mathrm{I}_0(h\,k)}}{64\frac{\mu_{nf}}{\mu_f}}, \tag{19}$$

$$\theta(r,z)=\frac{1}{4}\,\frac{k_f}{k_{nf}}\,(h^2-r^2)\beta, \tag{20}$$

$$\varphi=\xi\frac{\mathrm{I}_0(r\,k)}{\mathrm{I}_0(h\,k)}, \tag{21}$$

To find the pressure gradient, we use the flow rate in the moving frame given by:

$$F = 2\pi \int_0^h rw \; dr. \tag{22}$$

From equation (22), the pressure gradient can be obtained in terms of flow rate as follows:

$$\frac{dp}{dz} = \frac{7}{40} G_r \, L \, h^2 \frac{k_f}{k_{nf}} \, \beta + \frac{3 \, F}{h^3} \frac{\mu_{nf}}{\mu_f} + \frac{3\pi \, U \, \xi}{h^2 \mathrm{I}_0(h\,k)} [\mathrm{I}_1(h\,k) \, \mathrm{L}_0(h\,k) - \mathrm{I}_0(h\,k) \mathrm{L}_1(h\,k)], \tag{23}$$

where $\mathrm{I}_0(x), \mathrm{I}_1(x)$ are the modified Bessel function of the first kind, they are defined as follows:

$$\mathrm{I}_j(x) = \sum_{i=0}^{\infty} \frac{1}{i! \, \Gamma(i + j + 1)} \left(\frac{x}{2}\right)^{2i+j}, \tag{24}$$

and $\mathrm{L}_0(x), \mathrm{L}_1(x)$ are the modified Struve functions that are defined as:

$$\mathrm{L}_j(x) = \sum_{i=0}^{\infty} \frac{1}{i! \, \Gamma\left(\frac{3}{2} + i\right) \Gamma\left(\frac{3}{2} + i + j\right)} \left(\frac{x}{2}\right)^{2i+j+1}. \tag{25}$$

Using equation (23), we can evaluate the pressure rise ΔP as follows:

$$\Delta P = \int_0^1 \frac{dP}{dz} \, dz. \tag{26}$$

All the solutions are obtained with the help of Mathematical 11.0.

5. Results and Discussion

Using the thermo-physical characteristics of the base fluid and Cu-Water [32] as described below, we have plotted the graphs for the temperature, electric potential, velocity, and pressure distribution of the given problem.

Table 1: Thermo-physical properties of Pure water and Cu-water nanofluid.

Physical Properties	H_2O	Cu Water
$c_p(J/kgK)$	4179.0	385
$\rho(kg/m^3)$	997.1	8933

Temperature profile $\theta(r, z)$ has been plotted against the radial distance (Figure. 2), with variation in the nanoparticle volume fraction (φ) and heat source parameter (β). The graphical representation depicts that an increase in the amount of copper in the base fluid improves the thermal conductivity which cools down the fluid and thus the fluid temperature drops. Moreover, the smaller the heat source parameter, the lesser the temperature of the base fluid. Physically, low values of the heat source parameters mean that the intensity of the heat source is reduced, therefore, a reduction in temperature is noticed.

Electric potential $\varphi(r, z)$ is plotted against the radial distance (Figure. 3). We altered values of the Debye length parameter (k) and zeta potential (ξ) to evaluate the differences that they cause upon the electric potential and found that higher values of the Debye length parameter cause lower electric potential and higher values of boundary value parameter cause higher electric potential.

Velocity profile $w(r,z)$ is extensively studied and analyzed graphically (Figure. 4). It is observed that velocity has altogether different dynamics in the center of the tube and around the boundaries of the tube. At the center of the tube, velocity decreases as we increase either nanoparticle volume fraction, Debye length parameter, Helmholtz-Smoluchowski velocity and mean flow rate. On the other hand, an increase in velocity is observed as we increase the Grashof number and heat source parameter, which means that velocity is higher when the buoyancy forces are stronger than the viscous forces. This behavior of velocity reverses as we move from the center of the tube toward the boundaries of the tube.

Pressure gradient $\frac{dp}{dz}$ is examined against the axial distance (Figure. 5). We can see that the pressure gradient is less significant in the case of copper diluted water and greater in the case of plain pure water. This is due to the fact that the viscosity of the fluid increases with the addition of nanoparticles in the base fluid, so it requires more driving force. As a result, a decline in negative pressure gradient is produced. Moreover, the pressure gradient tends to rise as we increase either of the Debye length parameter, Grashof number, or the heat source parameter. Similarly, the Debye length parameter and Grashof number increase the pressure rise (Figure. 6). We note that as with the increase in the amount of copper in the base fluid (water), the pressure rise decreases in the augmented pumping region ($\Delta P < 0$) contrary to the peristaltic pumping region ($\Delta P > 0$).

Streamlines of the fluid flow are plotted (Figure. 7-9) to examine the movement of trapped boluses in the peristaltic flow phenomenon. We see that as the nanoparticle volume fraction increases, i.e. moving from pure water towards copper water, the number and size of the trapped bolus decreas. However, the opposite behavior of fluid flow can be seen in the case of the Grashof number and Debye length parameter which tend to increase the number and size of the trapped bolus.

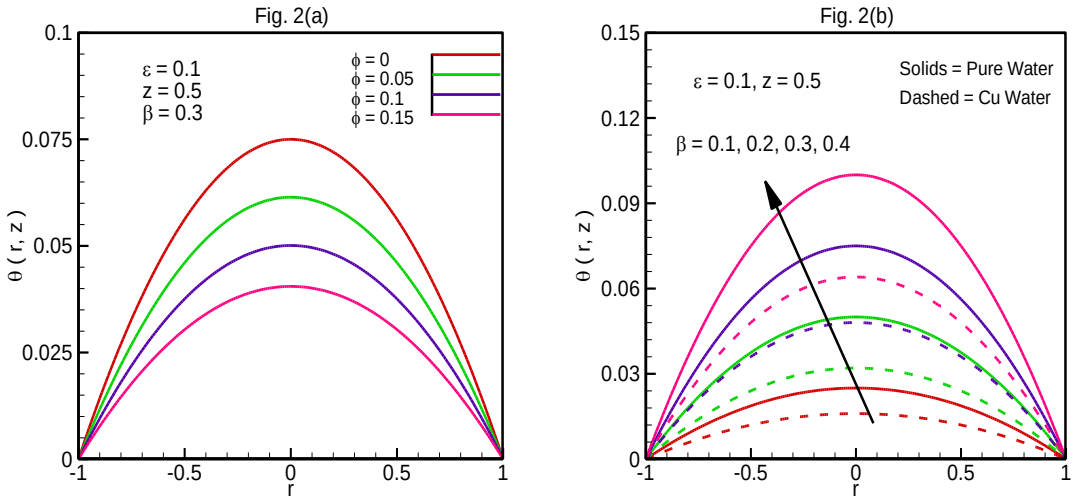

Figure 2: Temperature profile $\theta(r,z)$ is plotted alongside the radial distance r.

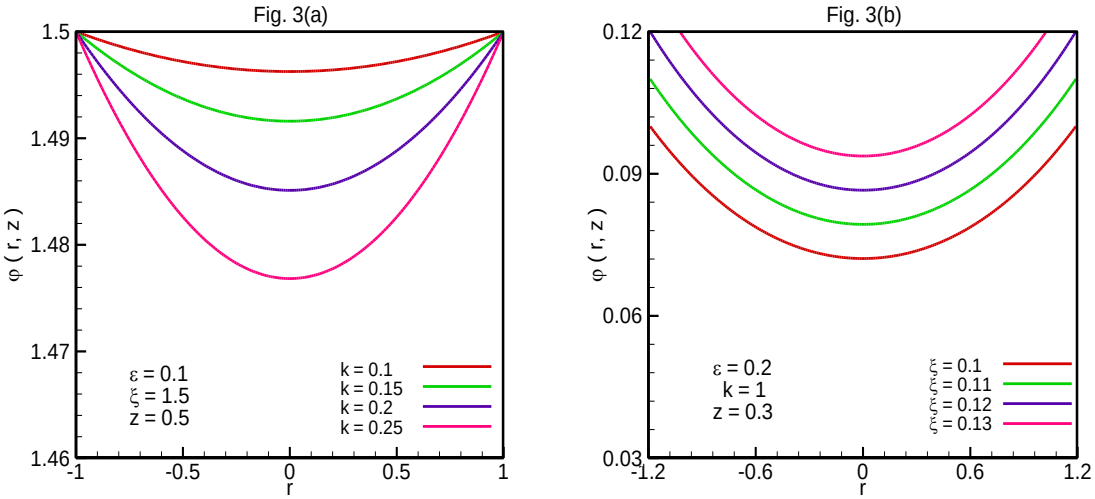

Figure 3: Electric potential $\varphi(r, z)$ is plotted alongside the radial distance r.

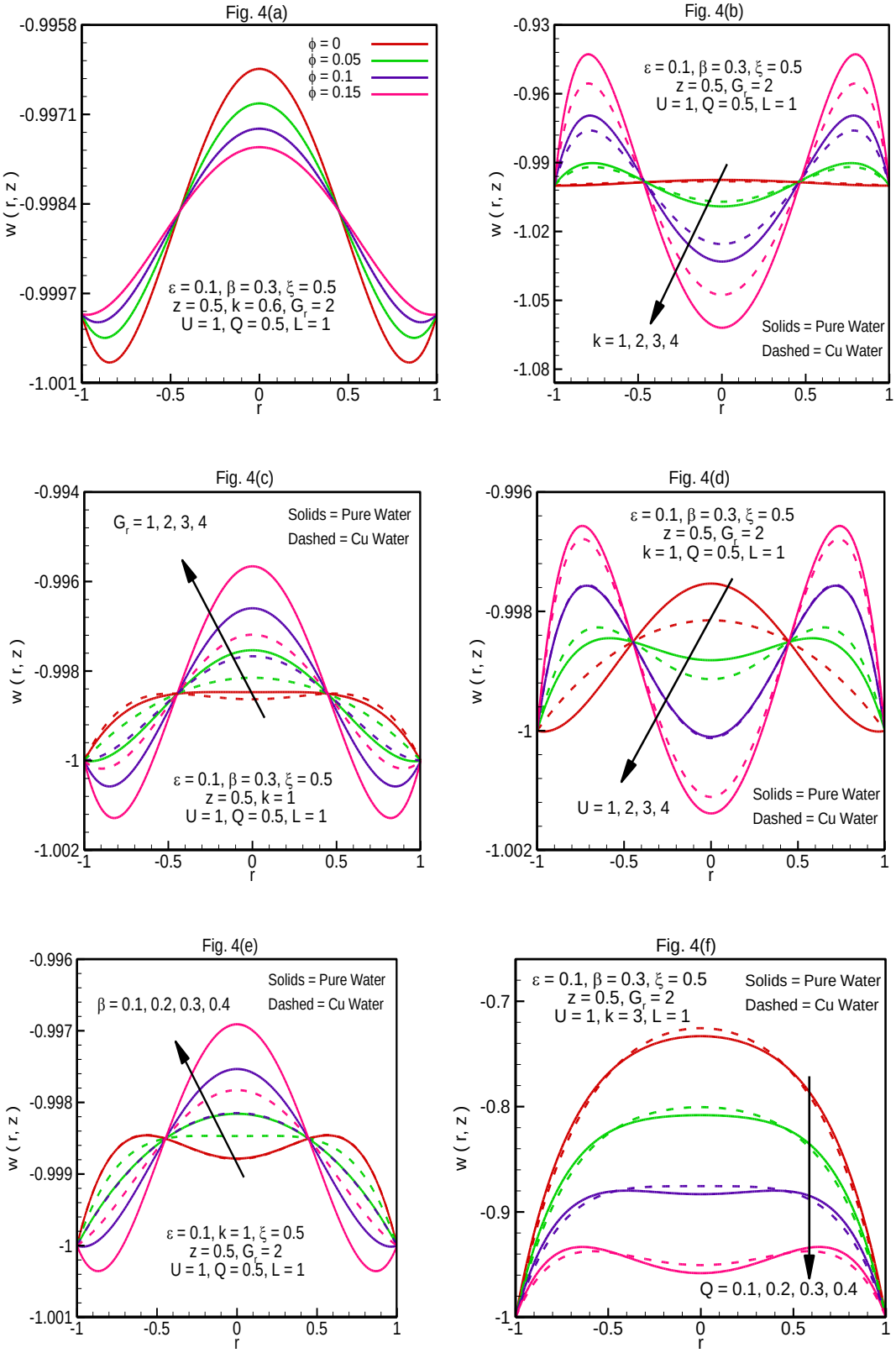

Figure 4: Velocity profile $w(r,z)$ is plotted alongside the radial distance r.

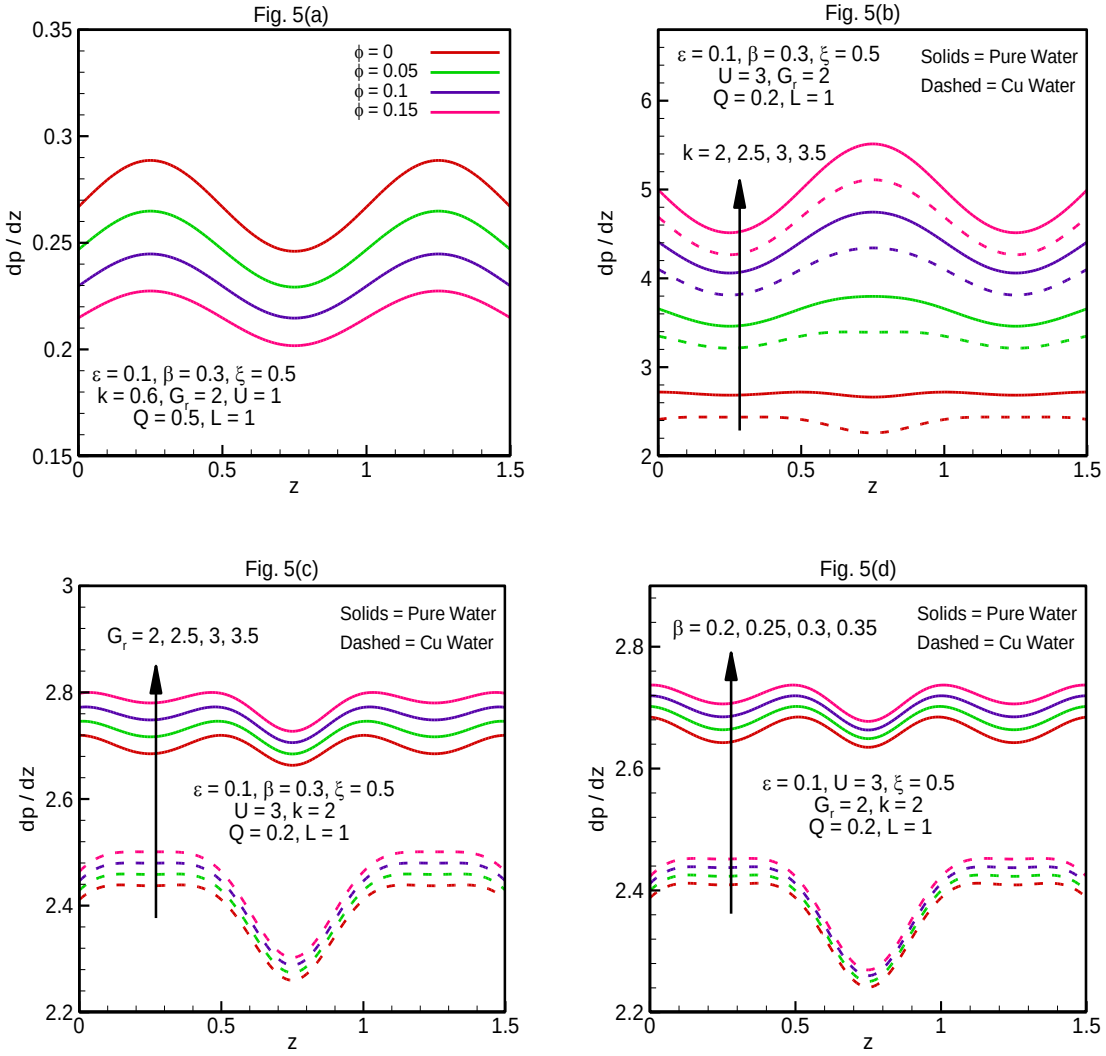

Figure 5: Pressure gradient $\frac{dp}{dz}$ is plotted alongside the axial distance z.

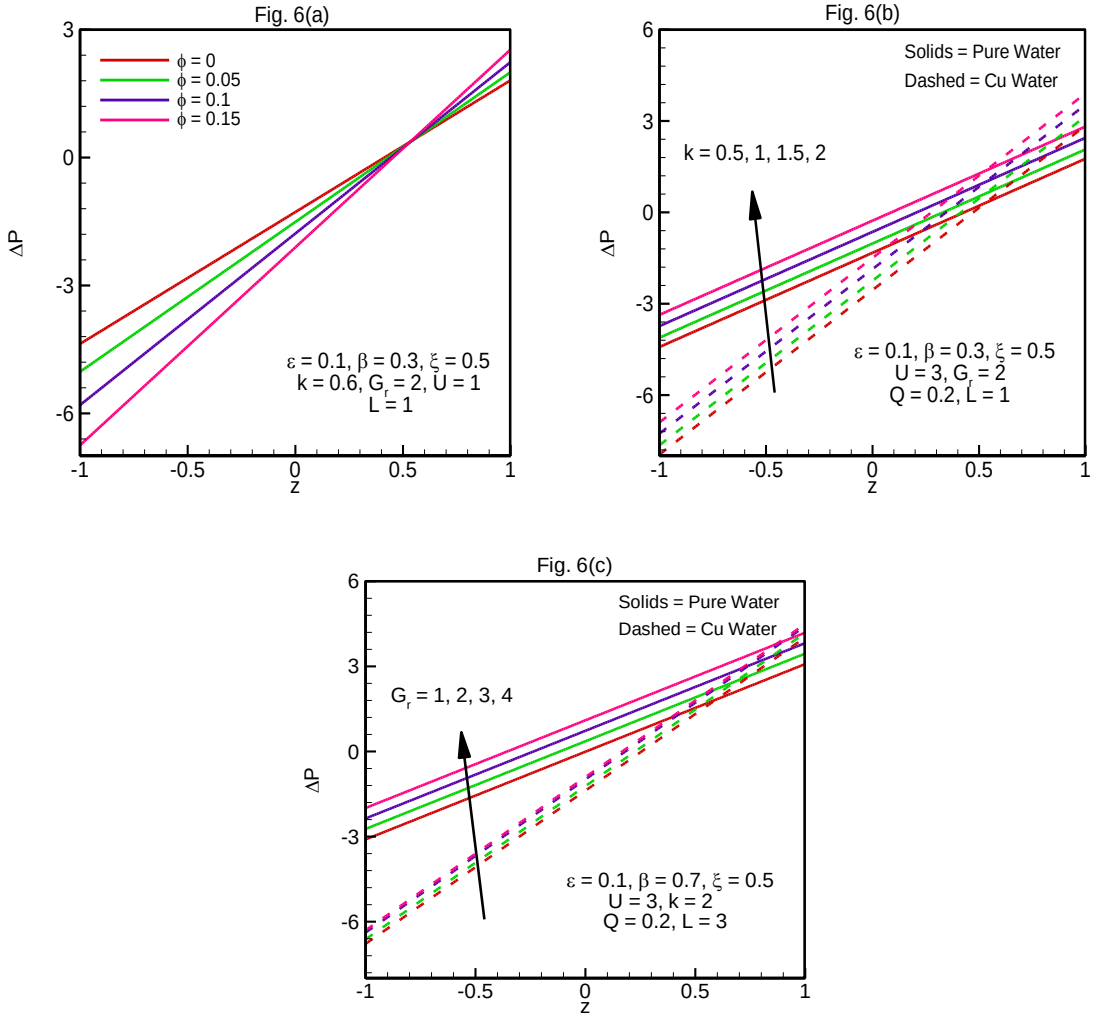

Figure 6: Pressure rise ΔP is plotted alongside the axial distance z.

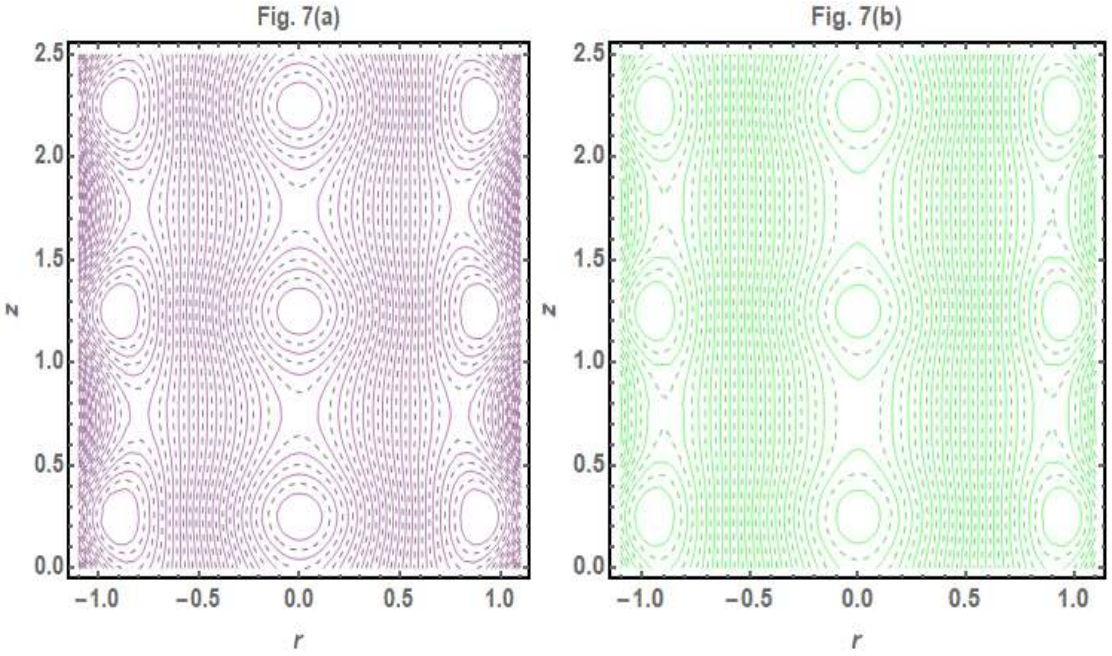

Figure 7: Streamlines for varying parameters $\phi = 0, 0.1$.

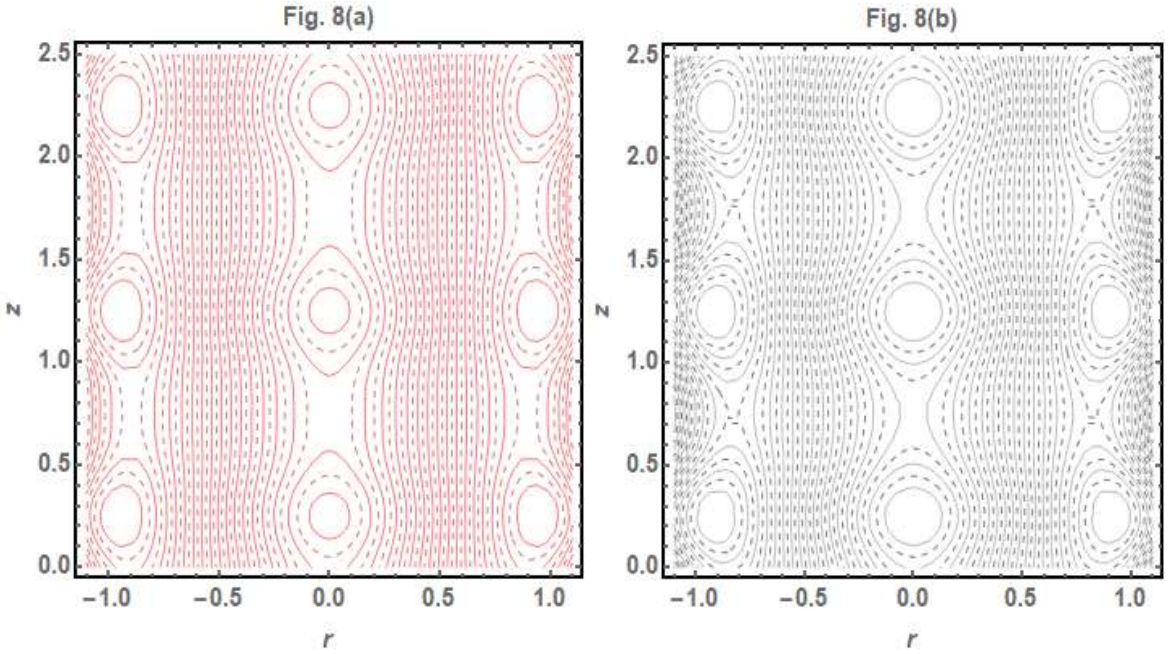

Figure 8: Streamlines for varying parameters $G_r = 2, 3$.

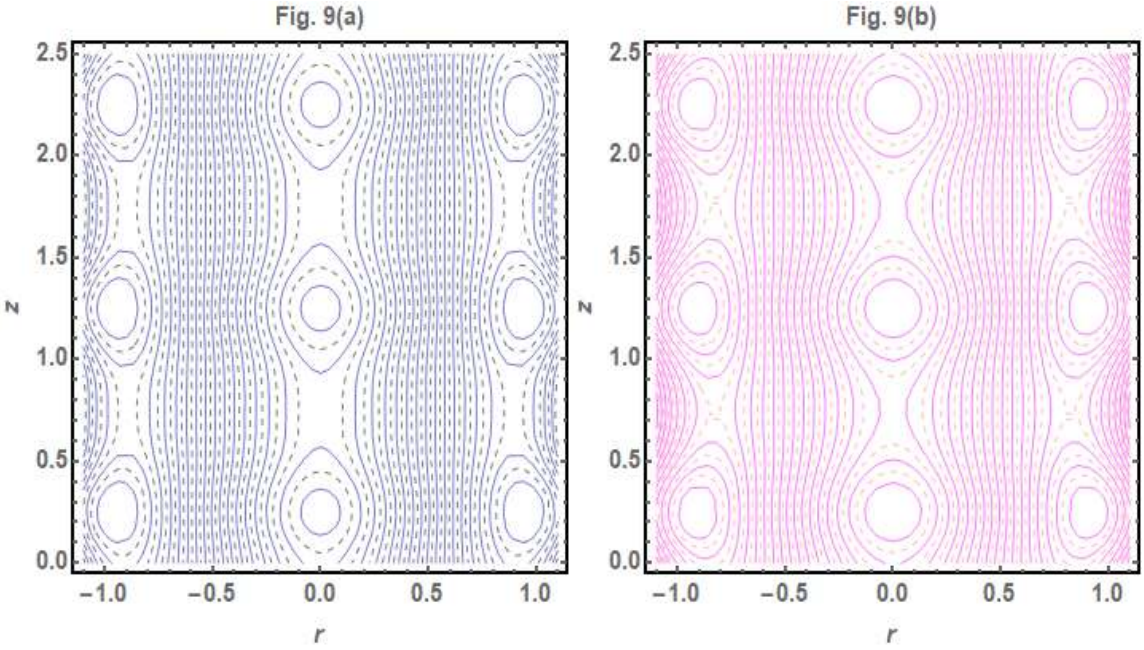

Figure 9: Streamlines for varying parameters $\beta = 0.2, 0.3$.

References

[1] S.L. Weinberg, E.C Eckstein, A. H. Shapiro, "An experimental study of peristaltic pumping," *J. Fluid Mech.* vol.49, no.3, pp. 461-479,1971.

[2] A.M. Provost, W.H. Schwarz," A theoretical study of viscous effects in peristaltic pumping," *J. Fluid Mech.* vol.279, pp.177-195, 1994.

[3] A.M. Rashad, T. Armaghani , A.J. Chamkha, M.A. Mansour, "Entropy Generation and MHD Natural Convection of a Nanofluid in an Inclined Square Porous Cavity: Effects of a Heat Sink and Source Size and Location," *Chin. J. Phys.* vol.56,no.1, pp. 193-211, 2018.

[4] M.M. Bhatti, A. Zeeshan, R. Ellahi, O.A. Bég, A. Kadir," Effects of coagulation on the two-phase peristaltic pumping of magnetized prandtl biofluid through an endoscopic annular geometry containing a porous medium," *Chin. J. Phys.* vol.58 , pp. 222–234, 2019.

[5] K.B. Vinayakumar, G. Nadiger, V.R. Shetty, N.S. Dinesh, M.M. Nayak, K. Rajanna," Packaged

peristaltic micropump for controlled drug delivery application," *Rev. Sci.* vol.88, no.1, pp. 015102, 2017.

[6] M.M. Bhatti, A. Zeeshan, N. Ijaz, "Slip effects and endoscopy analysis on blood flow of particle-fluid suspension induced by peristaltic wave," *J. Mol. Liq.* Vol.218, pp. 240-245, 2016.

[7] G.A. Longo, S. Mancin, G. Righetti, C. Zilio, "Flow dynamic and energetic assessment of a commercial micro-pump for a portable/wearable artificial kidney: Peristaltic vs. diaphragm pumps," *Therm. Sci. Eng. Prog.* Vol.3, pp. 31-36, 2017.

[8] D. Tripathi, S. Bhushan, O.A Bég, "Unsteady viscous flow driven by the combined effects of peristalsis and electro-osmosis," *Alex. Eng. J.* vol.57, no.3, pp. 1349-1359, 2018.

[9] F.F. Reuss, Sur un nouvel effet de l'électricité galvanique," *Mem. Soc. Imp. Natur. Moscou*, vol. 2, pp.327-337, 1809.

[10] H. Helmholtz, "Studien über elektrische Grenzflächen," *Ann. Phys. Chem., Neue Folge, vol.* 7, pp. 337-382, 1879.

[11] N.A. Patankar, H.H. Howard," Numerical simulation of electroosmotic flow, *Anal. Chem.* vol.70, no.9, pp. 1870-1881, 1998.

[12] J.G. Santiago," Electroosmotic flows in microchannels with finite inertial and pressure forces," *Anal. Chem* vol.73, no.10, pp. 2353-2365, 2001.

[13] P. Dutta, A. Beskok," Analytical solution of combined electroosmotic/pressure-driven flows in two-dimensional straight channels: finite Debye layer effects," *Anal. Chem.* vol.73, no.9, pp. 1979-1986,2001.

[14] D. Tripathi, J. Ravindra, O.A. Bég, S. Shaw," Electroosmosis modulated peristaltic biorheological flow through an asymmetric microchannel: a mathematical model," *Meccanica* vol.53, no.8, pp.2079-2090, 2018.

[15] A. Sharma D. Tripathi, R.K. Sharma, A.K. Tiwari, "Analysis of double-diffusive convection in electroosmosis regulated peristaltic transport of nanofluids," *Physica* A Stat. Mech. Appl. vol.535 , pp. 122-148, 2019.

[16] J. Prakash, K. Ramesh, D. Tripathi, R. Kumar," Numerical simulation of heat transfer in blood flow altered by electroosmosis through tapered micro-vessels," *Microvas. Res.* vol.118, pp.162-172, 2018.

[17] N.S. Akbar, S. Nadeem, T. Hayat, A. A. Hendi, "Peristaltic flow of a nanofluid in a non-uniform tube," *Heat Mass Transf.* vol.48,no.3, pp. 451-459, 2012.

[18] N. Bachok, A. Ishak, I. Pop, "Boundary-layer flow of nanofluids over a moving surface in a flowing fluid," *Int. J. Thermal Sci.* vol.49, no.9, pp. 1663-1668, 2010.

[19] S. Ganguly, S. Sarkar, T.K. Hota, M. Mishra," Thermally developing combined electroosmotic and pressure-driven flow of nanofluids in a microchannel under the effect of the magnetic field," *Chem. Eng. Sci.* vol.126, pp.10-21, 2015.

[20] N. Shehzad, A. Zeeshan, R. Ellahi," Electroosmotic flow of MHD power law Al2O3-PVC nanofluid in a horizontal channel: Couette-Poiseuille flow model," *Commun. Theor. Phys.* vol.69, no.6, pp. 655, 2018.

[21] J. Prakash, A. Sharma, D. Tripathi," Thermal radiation effects on electroosmosis modulated peristaltic transport of ionic nanoliquids in biomicrofluidics channel," *J. Mol. Liq.* Vol.249 , pp.843-855, 2018.

[22] A. Tanveer, M. Khan, T. Salahuddin, M.Y. Malik," Numerical simulation of electroosmosis regulated peristaltic transport of Bingham nanofluid, "*Comput. Meth. Prog. Biomed.* vol.180, pp. 105005, 2019.

[23] P. Jayavel, R. Jhorar, D. Tripathi, M.N. Azese, Electroosmotic flow of pseudoplastic nanoliquids via peristaltic pumping, *J. Braz. Soc. Mech. Sci. Eng.* vol.41,no.2,pp. 61, 2019.

[24] M. Mustafa, S. Hina, T. Hayat," A. Alsaedi, Influence of wall properties on the peristaltic flow of a nanofluid: analytic and numerical solutions," *Int. J. Heat Mass Transf.* vol.55, no.(17-18), pp. 4871-4877, 2012.

[25] D. Tripathi, O.A. Bég, A study on peristaltic flow of nanofluids: Application in drug delivery systems, *Int. J. Heat Mass Transf.* vol.70, pp: 61-70, 2014.

[26] J.Y. Qian, M.R. Chen, X.L. Liu, Z.J. Jin," A numerical investigation of the flow of nanofluids through a micro Tesla valve," *J. Zhejiang Univ. Sci A* vol.20,no.1, pp.50-60,2019.

[27] M.S. Liu, M.C.C. Lin, C.Y. Tsai, C.C. Wang, "Enhancement of thermal conductivity with Cu for

nanofluids using chemical reduction method," *Int. J. Heat Mass Transf.* vol.49, no.(17-18), pp. 3028-3033,2006.

[28] K. Vajravelu, K.V. Prasad, J. Lee, C. Lee, I. Pop, R.A.V. Gorder," Convective heat transfer in the flow of viscous Ag–water and Cu–water nanofluids over a stretching surface," *Int. J. Therm. Sci.* vol.50, no.5, pp. 843-851, 2011.

[29] K. Ramesha, M. Devakar," Effect of heat transfer on the peristaltic transport of a MHD second grade fluid through a porous medium in an inclined asymmetric channel," *Chin. J. Phys.* vol.55,no.3, pp. 825-844, 2017.

[30] K. Vajravelu, K.V. Prasad, NG Chiu-On, "The effect of variable viscosity on the flow and heat transfer of a viscous Ag-water and Cu-water nanofluid," *J. Hydrod.* vol.25, no.1, pp.1-9, 2013.

[31] D. Tripathi, S. Bhushan, O.A Bég, "Analytical study of electro-osmosis modulated capillary peristaltic hemodynamics," *J. Mech. Med. Biol.* vol.17, no.3, pp. 1750052, 2017.

[32] N.S. Akbar, A.W. Butt, "Bio mathematical venture for the metallic nanoparticles due to ciliary motion," *Comput. Method. Prog. BioMed.*, vol.134 , pp. 43-51, 2016.